



HAL
open science

Gas-phase acidity of D-glucose. A density functional theory study

Jean-Yves Salpin, Jeanine Tortajada

► **To cite this version:**

Jean-Yves Salpin, Jeanine Tortajada. Gas-phase acidity of D-glucose. A density functional theory study. *Journal of Mass Spectrometry*, 2004, 39 (8), pp.930-941. 10.1002/jms.671 . hal-00068618

HAL Id: hal-00068618

<https://hal.science/hal-00068618>

Submitted on 4 Oct 2018

HAL is a multi-disciplinary open access archive for the deposit and dissemination of scientific research documents, whether they are published or not. The documents may come from teaching and research institutions in France or abroad, or from public or private research centers.

L'archive ouverte pluridisciplinaire **HAL**, est destinée au dépôt et à la diffusion de documents scientifiques de niveau recherche, publiés ou non, émanant des établissements d'enseignement et de recherche français ou étrangers, des laboratoires publics ou privés.

Gas-phase acidity of D-glucose. A density functional theory study.

Jean-Yves Salpin and Jeanine Tortajada

Laboratoire Analyse et Environnement, UMR 8587, Bâtiment des Sciences, Université d'Evry Val d'Essonne, Boulevard François Mitterrand, 91025 EVRY CEDEX, France.

Corresponding author: Jean-Yves Salpin
Tel: 33 1 69 47 76 47 Fax: 33 1 69 47 76 55
e-mail : Jean-Yves.Salpin@chimie.univ-evry.fr

Number of pages (including Table and Figure legends) : **24**; Figures : **4**; Tables : **6**

Running title : DFT determination of D-glucose gas-phase acidity

Abstract

The gas-phase acidity of D-glucopyranose is studied by means of B3LYP calculations combined with 6-31G(d,p) or 6-31+G(d,p) standard basis sets. For each anomer, deprotonation of the various primary and secondary hydroxyl groups was considered. Like in solution, the anomeric hydroxyl is found to be the most acidic for both anomers, but only when the 6-31+G(d,p) basis set is used for geometry optimization. Deprotonation of the anomeric hydroxyl induces an important C(1)-O endocyclic bond elongation and subsequently promotes an energetically favored ring-opening process as attested by the very small calculated activation barriers. Our results also suggests that interconversion between the various deprotonated α and β anomers may easily occur under slightly energetic conditions.

B3LYP/6-311+G(2df,2p) calculations lead to the following absolute gas-phase acidities : $\Delta_{\text{acid}}G^{\circ}_{298}(\alpha\text{-D-glucose})= 1398 \text{ kJ}\cdot\text{mol}^{-1}$. This estimate matches nicely the only experimental value available to date. Finally, our study again confirms that use of diffuse functions on heavy atoms are necessary to properly describe anionic systems and to achieve good relative and absolute gas-phase acidities.

Keywords : DFT calculations, gas-phase acidity, D-glucose, mutarotation, ring-opening process

Introduction

Carbohydrates are the most abundant biomolecules in nature. They are mainly found as polysaccharides that play a crucial role in both animal and plant life. Cellulose for example is a structural component of vegetal cell walls, whereas starch or glycogen constitute food storage materials.¹ These three polysaccharides are homopolymers of D-glucose units bound together by different types of glycosidic linkages. The nature of the glycosidic bonds then influences both the structure and the role of these macromolecules, showing the fantastic diversity of carbohydrate chemistry.

Such a variety makes oligosaccharide analysis a challenging task for mass spectrometry. A complete structural description of carbohydrates implies exact mass measurement, sites and anomeric configuration of the glycosidic linkages, and also stereochemical characterization of the different asymmetric centers of the sugar ring. Many studies have been carried out on those topics for more than three decades, using different ionization techniques. It turned out that negative-ion mass spectrometry involving either chemical ionization², fast atom bombardment^{3,4,5} (FAB), Liquid Secondary Ion Mass Spectrometry^{6,7} (LSIMS) or Electrospray ionization^{8,9} (ESI), appeared particularly useful for the characterization of stereocenters and glycosidic linkages of both derivatized or underivatized oligosaccharides.

Recently Carroll *et al.*⁷ investigated the gas-phase fragmentation pathways of anionic oligosaccharides, and deduced from their experiments that cross-ring cleavage was facilitated by deprotonation of the anomeric oxygen, and subsequently was more favorable at the reducing end. As their findings suggested that the deprotonation site plays a key role in the fragmentation process, the authors performed AM1¹⁰ calculations on deprotonated β -D-glucose to determine the most acidic site of the molecule (the anomeric oxygen), and finally, proposed a mechanism accounting for the cross-ring cleavage. Apart from this particular work, the gas-phase acidity of D-glucose ions has been only scarcely studied^{11,12,13,14}, and all the calculations performed so far have not included any electron correlation during the

geometry optimization step. In addition, a striking result observed during our study about the gas-phase reactivity of lead(II) ions towards D-glucose¹⁵, was that the metallic center seemed to interact preferably with the deprotonated hydroxymethyl group, which is predicted to be the least acidic site according to the previous studies.^{7,11,12} For these different reasons, we found it necessary to reconsider the deprotonated D-glucose system at a higher level of calculation. Given the important size of these anions, we introduced electron correlation by using density functional theory (DFT) formalism. The advent of DFT methods has provided a cost-effective means for obtaining accurate thermochemical data and this paper presents the results obtained for both α and β anomers of D-glucose.

Computational details

Molecular orbital calculations have been carried out by using the B3LYP density functional approach, as implemented in the Gaussian-98 set of programs.¹⁶ This method combines Becke's three-parameter non local hybrid exchange potential¹⁷ with the non local correlation function of Lee, Yang and Parr.¹⁸ This particular hybrid functional has been found well suited for the study of inter- and intramolecular hydrogen bonds.^{19,20,21} Since it is well established^{22,23} that diffuse functions are very important to provide an adequate description of anionic systems, fully geometry optimization and vibrational analysis were performed with the double- ξ 6-31+G(d,p) basis set. Tight SCF convergence was systematically applied. For all the structures considered, a Natural Bond Orbital analysis²⁴ (NBO) has been carried out at this level by means of the NBO program.²⁵ Finally, relative energies were refined using the extended basis set 6-311+G(2df,2p). Searches for transition states were performed by choosing a single parameter (either bond length, bond angle or dihedral angle) as the reaction coordinate and by varying the coordinate serially, all other parameters being allowed to optimize. The resulting saddle points were confirmed by frequency calculations and the presence of a single negative eigenvalue.

Given the very large number of possible isomers for D-glucose, we have restricted our study to the most energetically preferred pyranosic 4C_1 conformation.

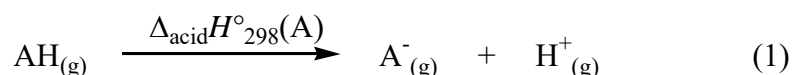
Throughout this paper total energies are expressed in hartree and relative energies in $\text{kJ}\cdot\text{mol}^{-1}$. Unless otherwise noted, the relative energies given hereafter are those obtained at the B3LYP/6-311+G(2df,2p)//B3LYP/6-31+G(d,p)+ZPE level. Detailed geometries of all the structures are available upon request.

Results

Reliability of the B3LYP/6-31+G(d,p) and B3LYP/6-311+G(2df,2p) levels for gas-phase acidity calculation

Proton transfer reactions are among the most studied processes in the gas-phase. Their thermochemistry is associated with two fundamental intrinsic properties of molecules, namely the proton affinity and the gas-phase acidity.

The gas-phase acidity of a given compound AH may be defined as the enthalpy change $\Delta_{\text{acid}}H^\circ_{298}(\text{A})$ for the following reaction :



Note that this term also corresponds to the proton affinity of the anionic counterpart A^- . During the last two decades, important progress in the development of both experimental and computational methods has resulted in a well-described gas-phase acidity scale. In this context, as density functional methods include explicitly electron correlation and are less computationally demanding than *ab initio* methods, several papers have addressed the question of their reliability to estimate gas-phase acidities.^{26,27,28,29} These studies have demonstrated that gas-phase acidities with an accuracy comparable to that achieved at high *ab initio* level (G2), could be obtained by using hybrid functionals like B3LYP or B3PW91, in combination with extended basis sets, such as 6-311+G(3df,2p)²⁶ or 6-311+G(3df,3pd).²⁸ Nevertheless, Burk et al.²⁹ have shown that the accuracy obtained with the commonly used

B3LYP functional, dramatically depends on the presence of diffuse functions, thus confirming that such functions are essential to describe the loosely bound extra electron of anionic species. Given the size of D-glucose, one cannot carry out for computational time considerations, calculations with basis sets as big as those previously mentioned. Instead, we opted for the B3LYP/6-31+G(d,p)+ZPE and B3LYP//6-311+G(2df,2p)//B3LYP/6-31+G(d,p)+ZPE levels. As the study of a complete series of acids is beyond the scope of the present paper, we chose to test the performance of these two levels with five molecules whose experimental gas-phase acidity is known with quite a good accuracy: H₂O, CH₃OH, C₂H₅OH, NH₃ and CH₃NH₂. The $\Delta_{\text{acid}}H^{\circ}_{298}$ terms have been estimated according to the following relationship (equation 1) :

$$\Delta_{\text{acid}}H^{\circ}_{298} = H^{\circ}_{298}(\text{A}^{-}) - H^{\circ}_{298}(\text{AH}) + \frac{5}{2} RT \quad (\text{eq. 1})$$

a $3/2RT$ component being considered for the proton translational energy. The results are listed in Table 1, together with the experimental values.^{30,31,32} Theoretical data include the unscaled zero-point energy (ZPE) and thermal correction to enthalpy both determined at the B3LYP/6-31+G(d,p) level of theory. For the sake of comparison, single point calculations have been also performed at the B3LYP/6-311++G(2df,2pd), which proved to give reliable acidities.²⁷ First, we can observe that whatever the level of calculation considered, the gas-phase acidities are in good agreement with the mean experimental values, with deviations ranging from 0 to 9 kJ.mol⁻¹. Addition of a *d* and a *f* polarization functions on heavy and hydrogen atoms, respectively, results in a significant decrease of the average absolute deviations $\bar{\Delta}$ (from 5.9 to 4.6 kJ.mol⁻¹). The use of extra diffuse and *d* polarization functions for hydrogen atoms further improves the accuracy ($\bar{\Delta} = 3.9$ kJ.mol⁻¹). Moreover, it is noteworthy that the most important deviations are observed for compounds which present experimental acidities with the largest uncertainties, suggesting that the gap might be due to some extent to the experimental data.

Mean absolute deviations calculated without considering ethanol, allow a straight comparison with the G2 results of Smith *et al*²⁶, who found a value of 2.3 kJ.mol⁻¹. This result is indeed better, but the G2 method cannot be applied to systems as big as hexoses. A similar uncertainty was obtained at the B3LYP/6-311+G(3df,2p) (2.2 kJ.mol⁻¹), a level which appears computationally too expensive for D-glucose, and consequently for bigger systems. In conclusion, our calculations show that the combination of the B3LYP functional with the 6-311+G(2df,2p) basis set gives good estimated gas-phase acidities. Finally, the B3LYP/6-31+G(d,p) level can be also used confidently for big systems, even if slightly less accurate than higher levels.

Relative gas-phase acidities of α and β -D-glucopyranose.

As already mentioned before, this study focuses on the ⁴C₁ pyranosic conformation of D-glucose and for each anomer, deprotonation of the five OH groups has been considered. In order to describe the cooperative intramolecular hydrogen bonding schemes within the different structures, we have used a six-letter descriptor which gives the orientation of the CH₂OH group, followed by that of the C(6), C(4), C(3), C(2) and finally C(1) secondary hydroxyls. The hydroxymethyl conformation is defined using the capital letters \bar{G} , G and T, and the hydroxyl conformations by the letters \bar{g} , g and t, as introduced by Cramer and Truhlar.³³ Each letter indicates whether the H-O(n)-C(n)-C(n-1) dihedral angle (or the O(6)-C(6)-C(5)-O(5) dihedral for CH₂OH) is gauche(-)[\bar{g} , \bar{G}], gauche(+) [g,G] or trans [t,T] (see Figure 1 for atomic labeling). For the present study, gauche(-) means that a counterclockwise (viewed in the O-to-C(n) direction) rotation of the OH (or CH₂OH) below or equal to 120° is required to eclipse the bond C(n)-C(n-1) (or C(5)-O), while for gauche(+), the rotation is clockwise. For dihedral angles greater than 120°, the trans orientation has been assigned. Finally, the letter x characterizes the deprotonated site, as introduced by Mulrone *et al*.¹²

With this convention, the $\alpha\mathbf{G1}$ structure depicted in Figure 1 is associated with the descriptor $\overline{\mathbf{G}}\overline{\mathbf{g}}\overline{\mathbf{g}}\overline{\mathbf{g}}\overline{\mathbf{x}}$.

For each alkoxide anion, the three commonly encountered hydroxymethyl conformations (G, $\overline{\mathbf{G}}$ and T) have been considered. Recently, Traeger and co-workers¹² noticed that the orientation of the anomeric hydroxyl was driven by the competition between the "exo-anomeric" effect³⁴ and the "negative" charge effect. The *exo*-anomeric effect is a stereoelectronic factor which induces a considerable barrier to rotation about the exocyclic C-O bond at the anomeric center. Anomeric axial or equatorial hydroxyl groups indeed prefer the gauche conformations ($\overline{\mathbf{g}}$ or \mathbf{g}) in which the electrons of one lone pair of the exocyclic O(1) oxygen are anti-periplanar with the C(1)-O(5) bond and thereby are delocalized into the endocyclic antibonding $\sigma^*_{\text{C(1)-O(5)}}$ bond orbital. On the other hand, the negative charge effect may be viewed as the tendency for the anomeric hydroxyl to participate in the cooperative hydrogen bonding scheme induced by a deprotonated hydroxyl and therefore to adopt a trans orientation. Consequently, for every anion and whatever the CH₂OH conformation, we have systematically considered the three possible orientations ($\overline{\mathbf{g}}$, \mathbf{g} or \mathbf{t}) for the anomeric OH group. Furthermore, in some cases, several additional conformations of OH(2) also had to be studied. The various anions have been labelled \mathbf{XYnp} according to the Cramer and Truhlar convention, where \mathbf{X} gives the anomeric form, \mathbf{Y} , the CH₂OH conformation. The letter \mathbf{n} gives the site of deprotonation and sometimes the corresponding anions will be referred to as "alkoxyn" species in the text. Finally, an additional letter (\mathbf{p}) is added when several anomeric conformations for the same anion are considered.

α -D-glucose.

B3LYP total and relative energies of the various structures examined for the α anomer are summarized in Table 2. The resulting relative gas-phase acidities are compared to those previously determined in Table 3. From this Table, we can see that the B3LYP energies

associated with the deprotonation of α -D-glucopyranose do not depend on the level of calculation. The anomeric hydroxyl is the most acidic and the following order of acidity is indeed obtained whatever the basis set used: OH(1) > OH(4) > OH(2) > OH(3) >> OH(6). The energy difference with the second most acidic site (OH(4)) is quite noticeable since we obtained a value of 11.6 kJ.mol⁻¹ (Table 3). A value of 12.4 kJ.mol⁻¹ is obtained at the B3LYP/6-311++G(2df,2p)//B3LYP/6-31++G(d,p)+ZPE level, suggesting that addition of diffuse functions on hydrogen atoms has a very minor effect on computed relative energies. Moreover, the primary hydroxyl (CH₂OH) is significantly less acidic than the secondary alcohols.

The most stable structures obtained at the B3LYP/6-31+G(d,p) level for each anion and neutral α -D-glucopyranose are presented in Figure 1. Whatever the deprotonation site, the structures obtained at the B3LYP/6-31G(d,p) and B3LYP/6-31+G(d,p) are very similar. Addition of a diffuse function only results in the lengthening of the various hydrogen bonds by ca 0.05-0.1 Å.

Deprotonation of the O(n)H (n=2-6) hydroxyl induces several important changes in the pyranosic ring, by lengthening the neighboring bonds. According to our NBO study and as already observed by Salzner et al.³⁵, this effect is attributed to hyperconjugation, that is delocalization of the lone pairs (LP) of the deprotonated oxygen into the σ anti-bonding orbitals of the following bonds: C(n)-H, C(n)-C(n-1) and C(n)-C(n+1). This n- σ^* electron transfer is also characterized by the important C(n)-O(n) shortening, typically of 0.06 Å.

In the particular case of the anomeric position (n=1, **α G1**), this negative charge effect competes with the *endo*-anomeric effect³⁶ which is caused by the interaction between the ring oxygen lone pairs and the antibonding $\sigma^*_{C(1)-O(1)}$ orbital and shortens the C(1)-O(5) endocyclic bond. Calculated NBO interaction energies E[LP_{O(1)}- $\sigma^*_{C(1)-O(5)}$] (negative charge effect) and E[LP_{O(5)}- $\sigma^*_{C(1)-O(1)}$] (*endo*-anomeric effect) are 174.6 kJ.mol⁻¹ and 29.5 kJ.mol⁻¹, respectively. So the negative charge effect completely counterpoises the *endo*-anomeric

effect, thereby increasing the C(1)–O(5) bond length by 0.132 Å compared to neutral α -D-glucose (Figure 1). It is also important to tackle the role of the strong O(2)–H \cdots O(1) hydrogen bond observed in the α G1 structure. This can be done for example by computing for anomeric alkoxide of 2-deoxy, 3-deoxy- and 4-deoxy- α -D-glucose the E[LP_{O(1)}- σ^* _{C(1)-O(5)}] NBO interaction energy. A complete conformational study of deoxy-D-glucoses being beyond the scope of this paper, this was achieved by just replacing in α G1 a hydroxyl group by a hydrogen atom for each position. The E[LP_{O(1)}- σ^* _{C(1)-O(5)}] interaction energy obtained for the 2-deoxy anomeric alkoxyde (246.6 kJ.mol⁻¹) is much greater than the value computed for α G1 structure (174.6 kJ.mol⁻¹). This results in a extremely activated C(1)–O(5) bond (1.633 Å), lengthened by 0.214 Å compared to neutral α -2-deoxy-D-glucose. Consequently, the strong O(2)–H \cdots O(1) hydrogen bond in α G1 anion strongly reduces the magnitude of the negative charge effect and allow its stabilization. Conversely, values obtained for 3-deoxy and 4-deoxy isomers (175.6 and 172.8 kJ.mol⁻¹, respectively) indicate that the O(3)–H \cdots O(2) and O(4)–H \cdots O(3) hydrogen bonds don't alter the negative charge effect.

B3LYP/6-31+G(d,p) calculations show that the most stable ⁴C₁ structure of neutral α -D-glucose exhibits a G hydroxymethyl conformation.³⁷ This is in agreement with ¹H NMR experiments carried out in aqueous solution³⁸, which demonstrated that less than 2% of T conformers are present. In the case of the gaseous anionic forms, the hydroxymethyl conformation depends on the deprotonation site (Table 2). The G orientation is favored when α -D-glucopyranose is deprotonated at the C(1) and C(2) hydroxyls (α G1 and α G2), whereas the CH₂OH group adopts a T conformation for deprotonation occurring at C(3), C(4) and C(6) hydroxyls (α T3, α T4 and α T6). These results are in agreement with the HF/6-31G(d) study of Mulroney et al.¹² This behaviour is promoted by the negative charge. Indeed, as we will see later, the cooperative intramolecular hydrogen bonding scheme is driven by the negative charge. As the negative charge comes up to the C(5) carbon, the CH₂OH group rotates to participate in the hydrogen bonding scheme induced by the charge. Two observations support

this assumption. First, $\alpha\mathbf{G-4}$ anions are much less stable than $\alpha\mathbf{T4}$ conformers (Table 2), whereas the energy difference between $\alpha\mathbf{G3}$ and $\alpha\mathbf{T3}$ is still small but already in favor of the T conformer. Secondly, $\alpha\mathbf{G-6}$ species do not correspond to minima on the potential energy surface as they spontaneously collapse to $\alpha\mathbf{T6}$ structures during the geometry optimization step.

Like the HF/6-31G(d) study carried out by Mulrone *et al.*¹², we found that the hydroxyl conformation of the anions is independent of the hydroxymethyl conformation. On the other hand, B3LYP/6-31+G(d,p) calculations lead to several differences. If the same orientation is observed for **alkoxy1** and **alkoxy2** anions, the DFT-optimized **alkoxy3** and **alkoxy4** ions exhibits *g x t t* and *x t t t* conformations, respectively, whereas the reported Hartree-Fock conformations are *g x t \bar{g}* and *x t t \bar{g}* . Consequently, the anionic oxygen is the driving force in determining the energetically preferred hydrogen bonding scheme whatever the site of deprotonation, while the *exo*-anomeric effects dominates for **alkoxy3** and **alkoxy4** ions at the HF/6-31G(d) level of theory.

Perturbation theory energy analysis of "donor-acceptor" interactions in the NBO basis can provide insight to rationalize the competition between the negative charge effect and the *exo*-anomeric effect. The first one is essentially characterized by the formation of a O(1)–H \cdots O(2) hydrogen bond whose strength is determined by the extent of delocalization of the O(2) lone pair(s) into the $\sigma^*_{\text{O(1)-H}}$ orbital. The second one is correlated to the $E[\text{LP}_{\text{O(1)}}-\sigma^*_{\text{C(1)-O(5)}}]$ interaction energy. The O(1)–H \cdots O(2) hydrogen bond in $\alpha\mathbf{G2}$, $\alpha\mathbf{T3}$ and $\alpha\mathbf{T4}$ is particularly strong as evidenced by the short distances obtained (1.864, 2.157 and 2.107 Å, respectively) and the particularly important $E[\text{LP}_{\text{O(2)}}-\sigma^*_{\text{O(1)-H}}]$ interaction energy (17.8, 14.4 and 18.3 kJ.mol⁻¹, respectively). One consequence of such strong interactions is that the lowest energy structures obtained at the HF/6-31G(d) level¹², which exhibit a \bar{g} anomeric conformation, do

not correspond to minima at the B3LYP/6-31+G(d,p) level as they systematically optimized to the t conformer (Table 2).

Rotation of OH(1) from t to g conformation for $\alpha\mathbf{G2}$, $\alpha\mathbf{T3}$ and $\alpha\mathbf{T4}$ structures results in the average increase of $E[\text{LP}_{\text{O}(1)}-\sigma^*_{\text{C}(1)-\text{O}(5)}]$ by ca 21 $\text{kJ}\cdot\text{mol}^{-1}$. But this additional *exo*-anomeric stabilization proves to be insufficient to counterbalance the stabilization provided by the hydrogen bond, all the more because the hydrogen bond due of its strength, induces an activation barrier to the rotation located 43 $\text{kJ}\cdot\text{mol}^{-1}$ above $\alpha\mathbf{G2}$ (and consequently only 1.2 $\text{kJ}\cdot\text{mol}^{-1}$ above $\alpha\mathbf{G2b}$). Moreover, the NBO study indicates that there are no hydrogen bonds between a gauche anomeric hydroxyl and the endocyclic oxygen. We can also notice that the energy gap between g and t conformers decrease from $\alpha\mathbf{G2}$ to $\alpha\mathbf{T4}$. The strength of the O(1)–H \cdots O(2) hydrogen bond appears therefore determinant in the preponderance of the charge effect over the *exo*-anomeric effect.

For **alkoxy4** anions with a g anomeric orientation, the O(2)H hydroxyl can exhibit two favorable conformations, $\bar{\text{g}}$ ($\alpha\mathbf{T4d}$) or t ($\alpha\mathbf{T4c}$) (see Table 2). For these two geometries, hydrogen bonds involving O(2) are of similar force. According to the NBO study the *exo*-anomeric effect is more pronounced for the t conformation. On the other hand, the *endo*-anomeric effect, monitored by the $E[\text{LP}_{\text{O}(5)}-\sigma^*_{\text{C}(1)-\text{O}(1)}]$ interaction energy, is more important when the O(2)H hydroxyl adopts a $\bar{\text{g}}$ conformation. The fact the $\alpha\mathbf{T4d}$ structure is slightly more stable than $\alpha\mathbf{T4c}$ suggest that the O(2)H orientation is correlated to the extent of the *endo*-anomeric effect.

Finally, we would like to make several comments concerning the deprotonation of the hydroxymethyl group. Stable geometries corresponding to **alkoxy6** species were very difficult to obtain. As already mentioned before, $\alpha\mathbf{G-6}$ species are not stable and converge to a $\alpha\mathbf{T6}$ species. This geometry is the only $\alpha\mathbf{T6}$ stable structure obtained and is characterized by a cooperative hydrogen bonding scheme induced by the *exo*-anomeric effect (Tx $\bar{\text{g}}\bar{\text{g}}\bar{\text{g}}\bar{\text{g}}$). The

O(4)–H··O(6) hydrogen bond is extremely strong, H··O(6) distance being 1.456 Å (Figure 1). On the other hand, when a "negative charge-induced" initial conformation (Tx t t t t) is considered, a proton transfer from O(6) to O(4) occurs during the optimization step.

β-D-glucose.

The lowest energy structures for the different alkoxy anions of β-D-glucopyranose are depicted in Figure 2. Total and relative energies of the various structures examined are summarized in Table 4. This table also includes calculations made at the B3LYP/6-31G(d,p) in order to discuss the influence of the diffuse functions. For a given deprotonation site, β forms are less stable than α forms. This is not surprising since α forms can be stabilized by two anomeric effects (both *endo* and *exo*) while the β forms can be stabilized only by one (*exo*).

The geometrical modifications induced by the deprotonation are similar to those previously described for the α anomer. In the particular case of the deprotonation of the anomeric center, the C(1)–O(5) bond elongation observed for the **βG1** form is more pronounced (0.143 Å) because the negative charge effect ($E[LP_{O(1)}-\sigma^*_{C(1)-O(5)}]=198.4 \text{ kJ.mol}^{-1}$) no longer competes with the *endo*-anomeric effect. Note that like for the α anomer, comparison with β-deoxy alkoxide ions demonstrate that the O2-H··O1 hydrogen bond plays a key role in the stabilization of the **βG1** anion, buy reducing the negative charge effect responsible for the strong C(1)-O(5) activation.

The hydroxymethyl orientation follows exactly the same trend than for the α anomer and does not have any influence on the cooperative hydrogen bonding scheme. Mulroney et al.¹² observed that like for the α-D-glucopyranose, the anomeric hydroxyl orientation was controlled by the *exo*-anomeric effect (*gauche* conformation) whatever the deprotonation site. Our B3LYP calculations lead to a different result for the **βG2** anion ($\bar{G}g\bar{g}\bar{g}xt$). This is

an other consequence of the competition between the negative charge effect and the *exo*-anomeric effect. The O(1)–H··O(2) hydrogen bond associated with the t conformer is strong for **βG2** as attested by its short length (2.162 Å, Figure 2) and the important E[LP_{O(2)}-σ*_{O(1)-H}] interaction energy (19.4 kJ.mol⁻¹), but is weak for **βT3b** and **βT4c** structures (2.414 and 2.287 Å and E[LP_{O(2)}-σ*_{O(1)-H}]=2.2 and 4.7 kJ.mol⁻¹, respectively). Rotation of OH(1) from t to g conformation for **βG2** does not lead to a stable structure (unlike HF/6-31G(d) calculations). On the other hand, the same rotation for **βT3b** and **βT4c** structures (leading to **βT3** and **βT4** species) results in the increase of E[LP_{O(1)}-σ*_{C(1)-O(5)}] by 32.4 and 33.4 kJ.mol⁻¹, respectively. If we compare the results obtained for both anomers, **αG2** and **βG2** are very similar in terms of interaction energy. The O(1)–H··O(2) hydrogen bond is strong for both structures and consequently the t orientation is preferred. Conversely, the situation is different for beta **alkoxy3** and **alkoxy4** anions. Unlike α forms, the O(1)–H··O(2) hydrogen bond is indeed weaker in the t orientation, while at the same time the *exo*-anomeric effect is more important in the g conformation. These two observations are both in favor of more stable g conformers, even if the energy gap between t and g conformers is rather small (Table 4).

Finally, in the case of **alkoxy4** anions, the most favorable orientation of OH(2) is trans when the anomeric hydroxyl is gauche (**βT4**, Tg x t t g). This can be attributed to the lack of *endo*-anomeric effect, which seems to play a key role in the energetically favored gauche orientation of the **αT4c** structure.

Whatever the deprotonation site, geometries obtained at the B3LYP/6-31G(d,p) and B3LYP/6-31+G(d,p) are very similar. However, examination of Table 3 points out the dramatic influence of the diffuse function on relative energies. The anomeric hydroxyl appears to be the most acidic site (like in solution³⁹) only when the 6-31+G(d,p) basis set is used in conjunction with the B3LYP functional. The following order of acidity is indeed obtained: OH(1) > OH(4) > OH(2) ≈ OH(3) >> OH(6). The acidity difference with the C(4)

hydroxyl is very small (2.6 kJ.mol^{-1}) and is unchanged when diffuse functions on hydrogen atoms are considered, while in solution the anomeric hydroxyl is believed to be considerably more acidic. As already underlined in several papers, our gas-phase study suggests that solvation may be the determining factor in the high acidity of the anomeric oxygen. Finally, like α anomer, stable geometries corresponding to **alkoxy6** species were very difficult to locate.

In summary, this DFT study establishes the anomeric hydroxyl as the most acidic site in the gas-phase for both anomers, but the difference in acidity with the other secondary hydroxyls groups is weak. Their orientation depends on three distinct effects, namely the negative charge effect, and the *endo* and *exo*-anomeric effects

Interconversion of the various deprotonated species.

In complement to this study, we have also explored the potential energy surface associated with the interconversion of the various deprotonated forms. This implies several proton transfers between adjacent hydroxyl group as well as hydroxymethyl rotation. For the β anomer, rotation of the anomeric hydroxyl has also to be considered since its orientation depends on the deprotonation site. Total and relative energies of the different transient species are given in Table 5. The resulting potential energy surfaces are represented in Figure 3 and 4 for α and β anomers, respectively. It turns out that the energy barriers associated with either 1,2 proton transfer or hydroxymethyl rotation are rather small. Starting from **alkoxy1** anion, the "proton ring walk" leading to the **alkoxy4** species only requires 50 kJ.mol^{-1} of internal energy. Therefore, such a process may readily occur in the source of a mass spectrometer under slightly energetic conditions, thus complicating gas-phase acidity measurements. This amount of energy may also be readily accessible in the long-lived ion-molecule complexes that must be generated when alkoxide ions are formed by proton transfer reactions.

These barrier heights are comparable to the G2(MP2) activation energies determined by Radom and co-workers for 1,2 hydride shifts within benzenium ions.⁴⁰ Barriers associated

with exocyclic hydroxymethyl rotation are rather small (24.8 and 28.4 kJ.mol⁻¹, for α and β anomers respectively) and are similar to those deduced from MP2/6-31G(d) calculations for neutral D-glucopyranose.^{41,42} Finally, a transition state for the rotation of the anomeric hydroxyl (TS11) from β T3b can be located but the corresponding energy barrier is negligible.

Ring opening processes.

It has been established that negative-ion mass spectrometry, and more particularly the unimolecular reactivity of (M-H)⁻ ions, was particularly helpful for characterization of stereocenters or glycosidic linkages of both derivatized or underivatized oligosaccharides.³⁻⁹ Structurally informative fragments are mostly associated with mechanisms involving cleavage of the pyranosic ring. Tandem mass spectrometry and isotopic labeling studies have been used previously to probe the fragmentations behavior of glucopyranosyl anions. In this context, several mechanisms (scheme 1) have been proposed to account for the ring-opening process, which is the first step of cross-ring cleavage.

<Scheme 1>

The first mechanism, suggested by Carroll et al.⁷ implies deprotonation of the anomeric position and cleavage of the C(1)-O(5) bond. The authors also specified that a cross-ring cleavage is no longer observed when the anomeric center is substituted. Promé et al.⁴ have shown that for glycosides pyranosic ring cleavage requires deprotonation of either C(4) or C(6) hydroxyls, followed by intramolecular attack on C(5) and cleavage of the C(5)-O(5) bond. So we investigated the energetics associated with these two mechanisms. For both anomers we considered that deprotonation could occur on the two most acidic sites and we tried to characterize the transition states and the resulting opened forms. Searches for transition states were performed by choosing a single parameter (either a bond length or a bond angle) as the reaction coordinate and by varying the coordinate serially. For ring-opening processes of **alkoxy1** structures, the C(1)-O(5) bond was lengthened while for

alkoxy4 structures the O(4)-C(4)-O(5) bond angle was progressively decreased. In both cases all other geometrical parameters were allowed to optimize.

Results are given in Table 5 and are illustrated by Figure 3 and 4. We can see that the ring-opening process from $\alpha\mathbf{G1}$ and $\beta\mathbf{G1}$ lead to a common opened form, **Open1** (Figure 3). The associated energy barriers are very low (+42.5 kJ.mol⁻¹) and decrease slightly when using a very extended basis set. These values are smaller than those obtained by AM1 for β -D-glucose⁷ (+73.2 kJ.mol⁻¹) and for D-cellobiose⁹ (+67.4 kJ.mol⁻¹). Consequently, cyclic species like $\alpha\mathbf{G1}$ and $\beta\mathbf{G1}$ may easily give acyclic anions under slightly energetic conditions. Moreover, these barriers may be readily accessible under low-energy MS/MS experiments. Finally, the reverse energy barriers are lower and the opened structure **Open1** is 38.1 kJ.mol⁻¹ higher in energy than $\alpha\mathbf{G1}$. Hence, a reversible $\alpha\mathbf{G1} \rightleftharpoons \beta\mathbf{G1}$ mutarotation process requires very little internal energy. A similar activation energy has been found recently for the mutarotation process in 2-tetrahydropyranol promoted by tautomeric catalysts.⁴³

Starting either from $\alpha\mathbf{T4}$ or $\beta\mathbf{T4}$, diminishing the O(4)-C(4)-O(5) bond angle actually activates the C(5)-O(5) elongation. However, the resulting opened forms (**Open3** and **Open4**) and the energy barriers associated with such intramolecular attacks are very high in energy (Figure 3 and 4), so that in the end these processes are much less favorable than those promoted by an anionic anomeric center (Figure 3). Formation of epoxy-like intermediate structures from pyranosic rings already proved to be unfavorable in the case of the Cu⁺/D-glucose system.⁴⁴ In conclusion, our calculations are consistent with the experimental data of Carroll et al.⁷ that show facile cross-ring cleavages when the anomeric position is not derivatized. Moreover the very facile mutarotation process allows the easy interconversion of α forms into β forms. For instance, the highest activation barrier associated with the $\alpha\mathbf{G1} \rightleftharpoons \beta\mathbf{T4}$ isomerization is only 50 kJ.mol⁻¹ above the $\alpha\mathbf{G1}$ species.

Absolute gas-phase acidity of D-glucopyranose.

Absolute gas-phase acidity $\Delta_{\text{acid}}H^{\circ}_{298}$ (defined by reaction 1) of each anomer may also be deduced from our calculations. By taking into account ZPE and thermal correction to enthalpy for the most stable structures of neutral and deprotonated D-glucose (αG1 , αglc , βG1 and βglc , see Figures 1 and 2), we found an absolute gas-phase acidity of α - and β -D-glucose equal to 1428 and 1438 kJ mol⁻¹, respectively, at the B3LYP/6-311+G(2df,2p)//B3LYP/6-31+G(d,p) level (Table 6). The free energy change of reaction (1) can be deduced from equation 2 :

$$\Delta_{\text{acid}}G^{\circ}_{298}(\text{AH}) = \Delta_{\text{acid}}H^{\circ}_{298}(\text{AH}) + T[\Delta_{\text{p}}S^{\circ}(\text{AH}) - S^{\circ}(\text{H}^+)] \quad (\text{eq. 2})$$

$\Delta_{\text{p}}S^{\circ}(\text{AH})$ being the protonation entropy of AH ($\Delta_{\text{p}}S^{\circ}(\text{AH})=S^{\circ}(\text{AH}) - S^{\circ}(\text{A}^-)$) and with $S^{\circ}(\text{H}^+) = 108.8 \text{ J.Mol}^{-1}.\text{K}^{-1}$.⁴⁵

The S° terms deduced from the vibrational analysis for the $\alpha\text{G1}/\alpha\text{glc}$ and $\beta\text{G1}/\beta\text{glc}$ pairs are comparable and we finally obtain $\Delta_{\text{acid}}G^{\circ}_{298}(\alpha\text{-D-glucose})= 1398 \text{ kJ.mol}^{-1}$ and $\Delta_{\text{acid}}G^{\circ}_{298}(\beta\text{-D-glucose})= 1408 \text{ kJ.mol}^{-1}$.

The thermochemistry associated with deprotonation of D-glucose is not well described experimentally. To date, only one experimental value has been reported in the literature. As part of their study dealing with attachment of small anions to neutral molecules, Cole and co-workers⁴⁶ examined the unimolecular reactivity of $[\text{M-H}]^{-\cdots} \text{H}^{\cdots}[\text{anion}]^{-}$ adducts and determined from the kinetic method that the $\Delta_{\text{acid}}G^{\circ}_{298}(\alpha\text{-D-glucose})$ falls in the range of 1374-1407 kJ mol⁻¹. A value of $1390 \pm 25 \text{ kJ mol}^{-1}$ can be obtained when the uncertainty associated with the reference gas-phase acidities are taken into account. Consequently, the calculated $\Delta_{\text{acid}}G^{\circ}_{298}(\alpha\text{-D-glucose})$ value is in good agreement with the experimental measurement, provided no significant entropy change is associated with the deprotonation process. Calculations carried out for D-glucose at the

B3LYP/6-311++G(2df,2p)//B3LYP/6-311++G(d,p)+ZPE give exactly the same $\Delta_{\text{acid}}H^{\circ}_{298}$ $\Delta_{\text{acid}}G^{\circ}_{298}$ value, confirming that inclusion of diffuse functions on hydrogen atoms has no effect on the computed values.

We have also estimated the absolute gas-phase acidity of 2-deoxy, 3-deoxy-, 4-deoxy- α -D-glucose and of 2-hydroxytetrahydropyran (referred to as 2-OH-THP). Results are given in Table 6. As already mentioned earlier, this was done by just replacing a hydroxyl group by a hydrogen atom for each position in order to compare values obtained with very similar geometries. As no conformational studies have been performed for these deoxy species, their presently estimated acidity do not intend to be accurate, but allow to address the role of the O(2)-H \cdots O(1) hydrogen bond on the absolute acidity. For example, the calculated $\Delta_{\text{acid}}G^{\circ}_{298}$ for 2-OH-THP differs significantly from the experimental value determined by Baer et al.⁴⁷ by ion-molecule reaction bracketing (1469 kJ.mol⁻¹).

Adding hydroxyl groups logically exalts the acidity (decrease of both $\Delta_{\text{acid}}H^{\circ}_{298}$ and $\Delta_{\text{acid}}G^{\circ}_{298}$ by ca 85 kJ.mol⁻¹ between 2-OH-THP and D-glucose). Taking D-glucose as a reference, examination of the variations show that the acidity strongly decreases when OH(2) is replaced by a hydrogen atom. A variation of ca 40 kJ.mol⁻¹ is indeed observed while removal of either OH(3) or OH(4) induces only a slight decrease. This is an other consequence of the anomeric alkoxide stabilization by the O(2)-H \cdots O1 hydrogen bond. Furthermore, this hydrogen bond seems to play a role in the higher acidity of the α anomers.

Conclusion

B3LYP hybrid functional in combination with the 6-31+G(d,p) and 6-311+G(2df,2p) basis sets gives reliable relative and absolute gas-phase acidities. However, the accuracy dramatically depends on the presence of a diffuse function, thus confirming that such a function is essential to describe the loosely bound extra electron of anionic species.

In the case of D-glucose, the anomeric hydroxyl is found to be the most acidic for both anomers, but only when the 6-31+G(d,p) basis set is used for geometry optimization. NBO analysis of the B3LYP wave functions confirm that the various effects (negative charge, *exo*- and *endo*-anomeric) responsible for the hydroxyl orientations are due to hyperconjugation. Deprotonation of the anomeric hydroxyl induces a very facile ring-opening process due to the important C(1)-O endocyclic bond. Moreover, interconversion between deprotonated α and β anomers through the **open1** structure may easily occur under slightly energetic conditions.

B3LYP/6-311+G(2df,2p) calculations lead to the following absolute gas-phase acidities : $\Delta_{\text{acid}}G^{\circ}_{298}(\alpha\text{-D-glucose})= 1398 \text{ kJ.mol}^{-1}$ and $\Delta_{\text{acid}}G^{\circ}_{298}(\beta\text{-D-glucose})= 1408 \text{ kJ.mol}^{-1}$. These estimates match nicely the only available experimental value determined for the α -anomer.

Acknowledgements

The authors would like to thank the Institut du Développement et des Ressources en Informatique Scientifique (IDRIS, CNRS) for computational time.

Table and Figure Caption

Table 1 : Calculated enthalpies H°_{298} (Hartree), B3LYP and experimental deprotonation enthalpies $\Delta_{\text{acid}}H^{\circ}_{298}$ (kJ.mol^{-1}).

Table2 : Total (Hartree), ZPE (kJ.mol^{-1}) and relative energies (kJ.mol^{-1}) of the different deprotonated structures of α -D-glucose.

Table3 : Summary of semi-empirical, *ab initio* and DFT relative energies (kJ.mol^{-1}) for the lowest energy structures of D-glucopyranose.

Table 4: Total (Hartree), ZPE (kJ.mol^{-1}) and relative energies (kJ.mol^{-1}) of the different deprotonated structures of β -D-glucose.

Table 5: Total (Hartree), ZPE ($\text{kJ}\cdot\text{mol}^{-1}$) and relative energies ($\text{kJ}\cdot\text{mol}^{-1}$) of opened forms and transition states associated with isomerization of deprotonated D-glucose

Table 6 : B3LYP/6-311+G(2df,2p)//B3LYP/6-31+G(d,p) $\Delta_{acid}\text{H}^{\bullet}_{298}$ and $\Delta_{acid}\text{G}^{\bullet}_{298}$ ($\text{kJ}\cdot\text{mol}^{-1}$) of α - and β - anomers of D-glucose and deoxy-D-glucoses (see text for details).

Figure 1 : B3LYP/6-31+G(d,p) geometries of the lowest energy structures of neutral and deprotonated α -D-glucopyranose.

Figure 2 : B3LYP/6-31+G(d,p) geometries of the lowest energy structures of neutral and deprotonated β -D-glucopyranose.

Figure 3 : B3LYP/6-311+G(2df,2p) potential energy surface for the interconversion of the different deprotonated forms α -D-glucopyranose

Figure 4 : B3LYP/6-311+G(2df,2p) energy diagram for the interconversion of the different deprotonated forms β -D-glucopyranose

References and notes

1. Lehninger AL, Nelson DL, Cox MM Principes de biochimie (2nd ed). Flammarion: Paris; 1994.
2. Cole RB, Tabet JC, Salles C, Jallageas JC, Crouzet J. Structural Memory Effects Influencing Decompositions of Glucose Alkoxide Anions Produced from Monoterpene Glycoside Isomers in Tandem Mass Spectrometry. *Rapid Commun. Mass Spectrom.* 1989;**3**:59-61.
3. Dell A, Ballou CE. Fast-atom-Bombardment, negative-ion mass spectrometry of the mycobacterial O-methyl-D-glucose polysaccharide and lipopolysaccharides. *Carbohydr. Res.* 1983;**120**:95-111.
4. Promé JC, Aurelle H, Promé D, Savagnac A. Gas-Phase glycosidic cleavage of Oxyanions from Alkyl Glycosides. *Org. Mass Spectrom.* 1987;**22**: 6-12.
5. Garozzo D, Giuffrida M, Impallomeni G, Ballistreri A, Montaudo G. Determination of linkage position and identification of the reducing linear oligosaccharides by negative ion fast atom bombardment mass spectrometry. *Anal. Chem.* 1990;**62**:279-286.
6. Carroll JA, Ngoka L, Lambert CG, Lebrilla CB. Liquid secondary ion mass spectrometry/Fourier transform mass spectrometry of oligosaccharide anions. *Anal. Chem.* 1993;**65**:1582-1587.
7. Carroll JA, Willard D, Lebrilla CB. Energetic of cross-ring cleavages and their relevance to the linkage determination of oligosaccharides. *Anal. Chim. Acta* 1995;**307**:431-447.
8. Garozzo D, Impallomeni G, Spina E, Green BN, Hutton T. Linkage Analysis, in Disaccharides by Electrospray Mass Spectrometry. *Carbohydr. Res.* 1991;**221**:253-257.
9. Mulroney B, Traeger JC, Stone BA. Determination of Both Linkage position and anomeric configuration in underivatized Glucopyranosyl Disaccharides by Electrospray mass Spectrometry. *J. Mass Spectrom.* 1995;**30**:1277-1283.
10. Dewar MJS, Zoebisch EG, Healy EF; Stewart, JJP. AM1: A New General Purpose Quantum Mechanical Molecular Model. *J. Am. Chem. Soc.* 1985;**107**:3902-3909

-
- 11 Brewster ME, Huang M, Pop A, Pitha J, Dewar MJS, Kaminski JJ, Bodor N. An AM1 molecular orbital study of α -D-glucopyranose and β -D-maltose : evaluation and implications. *Carbohydr. Res.* 1993; **242**:53-67.
 - 12 Mulrone B, Peel JB, Traeger JC, Stone BA. Relative gas phase acidities of D-glucopyranose from molecular Orbital Calculations. *J. Mass Spectrom.* 1999; **34**: 544-553.
 - 13 Carroll JA, Willard D, Lebrilla CB. Energetics of cross-ring cleavages and their relevance to the linkage determination of oligosaccharides. *Anal. Chim. Acta* 1995;**307**: 431-447.
 - 14 Cai Y, Concha MC, Murray JS, Cole RB. Evaluation of the role of multiple hydrogen bonding in offering stability to negative ion adducts in electrospray mass spectrometry. *J. Am. Soc. Mass Spectrom.* 2002;**13**:1360-1369.
 - 15 Salpin JY, Tortajada J. Gas-phase reactivity of Lead(II) ions with D-glucose. A combined electrospray ionization mass spectrometry and theoretical study. *J. Phys. Chem. A* 2003; **107**, 2943-2953.
 - 16 Gaussian 98, Revision A.7, Frisch MJ, Trucks GW, Schlegel HB, Scuseria GE, Robb MA, Cheeseman JR, Zakrzewski VG, Montgomery Jr. JA, Stratmann RE, Burant JC, Dapprich S, Millam JM, Daniels AD, Kudin KN, Strain MC, Farkas O, Tomasi J, Barone V, Cossi M, Cammi R, Mennucci B, Pomelli C, Adamo C, Clifford S, Ochterski J, Petersson GA, Ayala PY, Cui Q, Morokuma K, Malick DK, Rabuck AD, Raghavachari K, Foresman JB, Cioslowski J, Ortiz JV, Baboul AG, Stefanov BB, Liu G, Liashenko A, Piskorz P, Komaromi I, Gomperts R, Martin RL, Fox DJ, Keith T, Al-Laham MA, Peng CY, Nanayakkara A, Gonzalez C, Challacombe M, Gill PMW, Johnson B, Chen W, Wong MW, Andres JL, Gonzalez C, Head-Gordon M, Replogle ES, Pople JA. Gaussian, Inc., Pittsburgh PA, 1998.
 - 17 Becke, AD. Density-functional thermochemistry. III. The role of exact exchange. *J. Chem. Phys.* 1993; **98**: 5648-5652.

-
18. Lee C, Yang W, Parr RG. Development of the Colle-Salvetti correlation-energy formula into a functional of the electron density. *Phys. Rev. B Condens. Matter* 1988;**37**:785-789.
 19. González L, Mó O, Yáñez M. High-level ab initio versus DFT calculations on (H₂O₂)₂ and H₂O₂-H₂O complexes as prototypes of multiple hydrogen bond systems. *J. Comput. Chem.* 1997;**18**:1124-1135.
 20. González L, Mó O, Yáñez M. High-Level ab Initio Calculations on the Intramolecular Hydrogen Bond in Thiomalonaldehyde. *J. Phys. Chem. A* 1997;**101**:9710-9719.
 21. González L, Mó O, Yáñez M. High level ab initio and density functional theory studies on methanol-water dimers and cyclic methanol(water)₂ trimer. *J. Chem. Phys.* 1998;**109**:139-150.
 22. Clark T, Chandrasekhar J, Spitznagel GW, von-Rague-Schleyer P. Efficient diffuse function-augmented basis sets for anion calculations. III. The 3-21+G basis set for first-row elements Li-F. *J. Comput. Chem.* 1983;**4**, 294-301.
 23. Foresman JB, Frisch AE. Exploring Chemistry with electronic structure methods, Second Edition. Gaussian, Inc. Pittsburgh, PA, 1996.
 24. Reed AE, Curtiss LA, Weinhold F. Intramolecular interactions from a natural bond orbital, donor-acceptor viewpoint. *Chem. Rev.* 1988;**88**, 899-926.
 25. Glendening ED, Reed AE, Weinhold F. NBO version 3.1.
 26. Smith BJ, Radom L. Gas-phase acidities : a comparison of density functional, MP2, MP4, F4, G2(MP2,SVP), G2(MP2), and G2 procedures. *Chem. Phys Lett.* 1993;**245**:123-128.
 27. Merrill GN, Kass SR. Calculated Gas-Phase acidities Using Density Funtional Theory : Is it reliable ? *J. Phys. Chem.* 1996;**100**:17465-17471.
 28. Catalán J, Palomar J. Gas-Phase protolysis between neutral Brønsted acid and a neutral Brønsted base ? *Chem. Phys. Letters* 1998;**293**:511-514.
 29. Burk P, Koppel IA, Koppel I, Leito I, Travnikova O. Critical test of performance of B3LYP functional for prediction of gas-phase acidities and basicities. *Chem. Phys. Lett.* 2000;**323**:482-489.

-
- 30 Berkowitz J, Barney Ellison G, Gutman D. Three methods to measure RH bond energies. *J. Phys. Chem.* 1994;**98**:2744-2765.
- 31 NIST Chemistry Webbook, NIST standard reference database number 69 (2000), <http://webbook.nist.gov/chemistry>
- 32 Ervin KJM, DeTuri VF. Anchoring the gas-phase acidity scale. *J. Phys. Chem. A* 2002;**106**:9947-9956.
33. Cramer CJ, Truhlar DG. Quantum chemical conformational analysis of glucose in aqueous solution. *J. Am. Chem. Soc.* 1993;**115**:5745-5753.
- 34 Lemieux RU, Pavia AA, Martin JC, Watanabe KA. Solvation effects on conformational equilibria. Studies related to the conformational properties of 2-methoxytetrahydropyrans and related methyl glucopyranosides. *Can. J. Chem.* 1969;**47**:4427-4439.
- 35 Salzner U, von Ragué Schleyer P. Ab initio examination of anomeric effects in tetrahydropyrans, 1,3-dioxanes, and glucose. *J. Org. Chem.* 1994;**59**:2138-2155.
- 36 Edward JT. Stability of glycosides to acid hydrolysis. *Chem. Ind.* 1955;1102-1104.
37. Salpin JY. Unpublished results.
- 38 Nishida Y, Ohruai H, Meguro H. ¹H-NMR studies of (6r)- and (6s)-deuterated D-hexoses: assignment of the preferred rotamers about C5–C6 bond of D-glucose and D-galactose derivatives in solutions. *Tetrahedron Lett.* 1984;**25**:1575-1578.
- 39 Goud RF. Carbohydrates in Solution Vol. 117. American Chemical Society. Washington DC;1971.
- 40 Glukhovtsev MN, Mikhail N, Pross A, Nicolaidis A, Radom L. Is the most stable gas-phase isomer of the benzenium cation a face-protonated π -complex ? *J. Chem. Soc. Chem. Commun.* 1995;**22**:2347-2348.
- 41 Brown JW, Wadlowski BD. Ab initio studies of the exocyclic hydroxymethyl rotational surface in α -D-glucopyranose. *J. Am. Chem. Soc.* 1996;**118**:1190-1193.

-
- 42 Wadlowski BD, Chenoweth SA, Jones KE, Brown JW. Exocyclic hydroxymethyl rotational conformers of β - and α -D-glucopyranose in the gas-phase and in aqueous solution. *J. Phys. Chem. A* 1998;**102**:5086-5092.
- 43 Morpurgo S, Bossa M. The epimerisation of 2-hydropyranol catalysed by the tautomeric couples 2-pyridone/2-hydroxypyridine and formamide/formamidic acid as a model for the sugar's mutarotation: a theoretical study. *Phys. Chem. Chem. Phys.* 2003;**5**:1181-1189.
- 44 Alcamí M, Luna A, Mó O, Yáñez M, Boutreau L, Tortajada J. Experimental and Theoretical Investigation of the Reactions between Glucose and Cu^+ in the Gas Phase. *J. Phys. Chem. A* 2002;**106**:2641-2651.
- 45 Loewenschuss A, Marcus Y. The entropies of polyatomic gaseous ions. *Chem. Rev.* 1984;**84**:89-115.
- 46 Cai Y, Cole RB. Stabilization of anionic adducts in negative ion electrospray mass spectrometry. *Anal. Chem.* 2002;**74**:985-991.
- 47 Baer S, Brinkman EA, Brauman JI. Hemiacetal anions: A Model for tetrahedral reaction intermediates. *J. Am. Chem. Soc.* 1991;**113**:805-812.

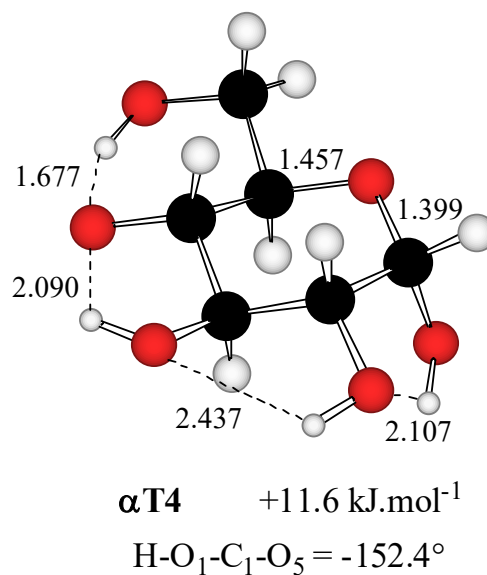
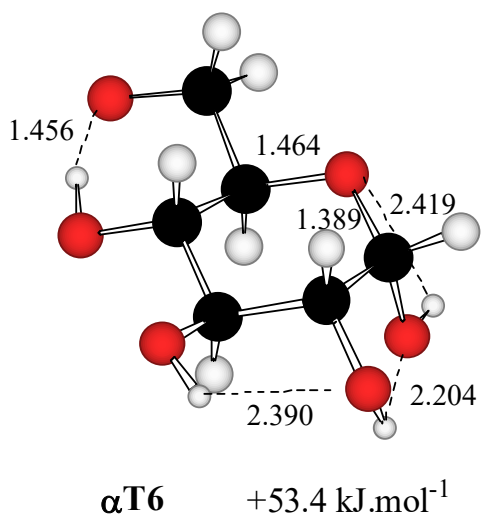
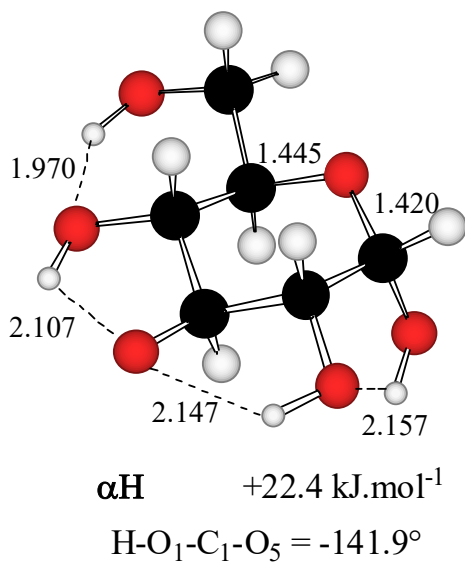
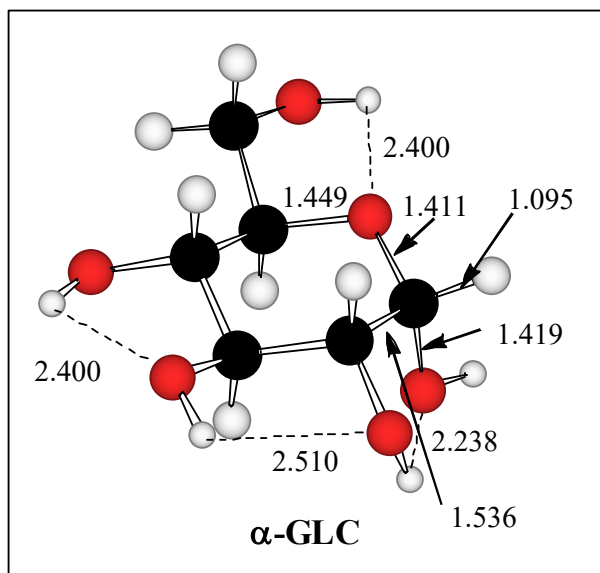
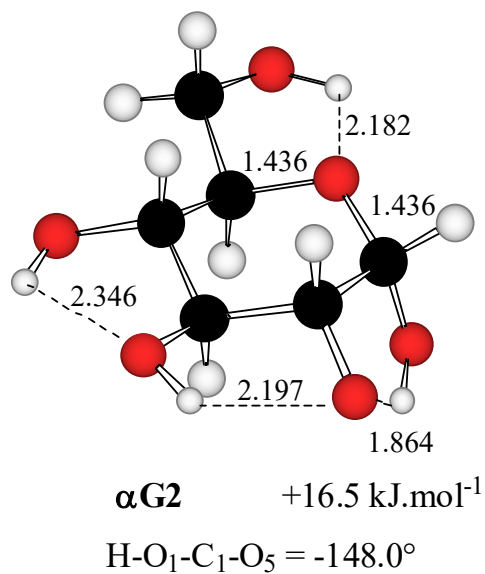
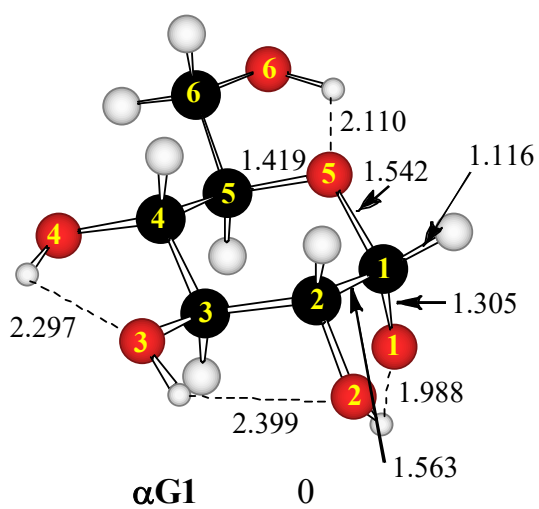


FIGURE 1

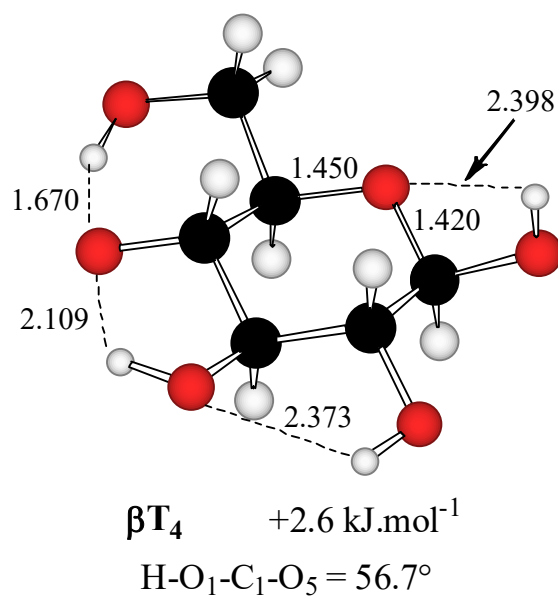
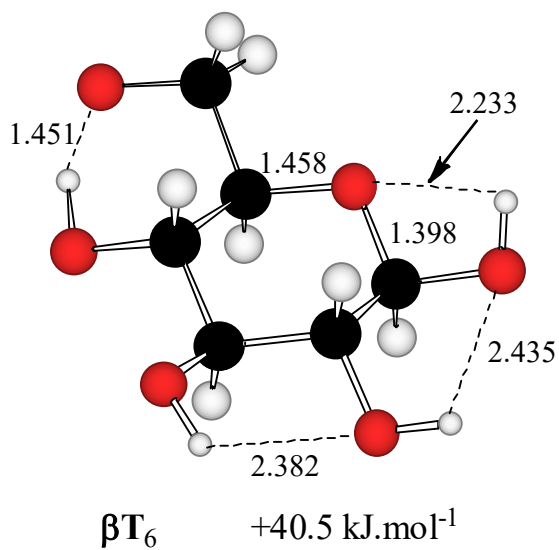
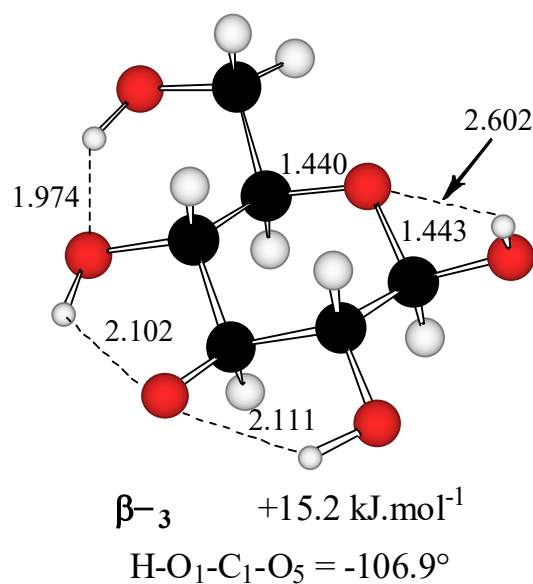
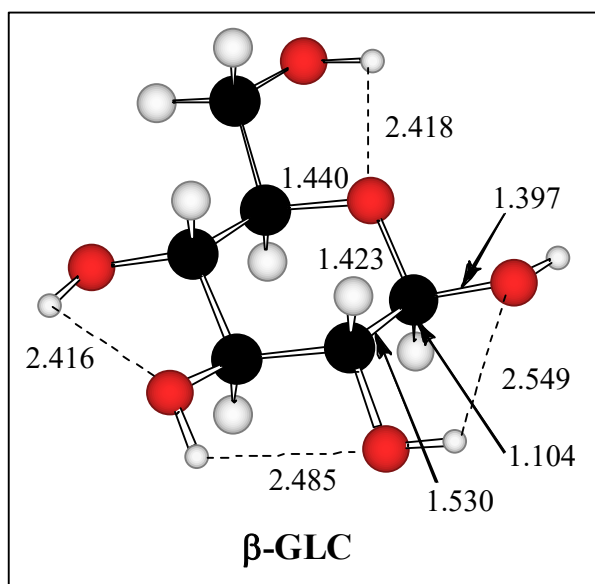
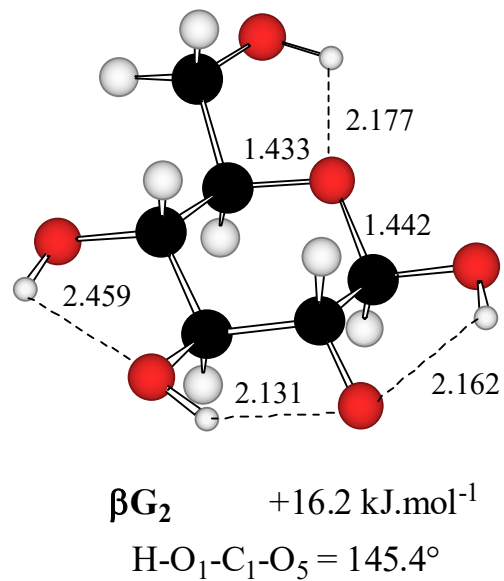
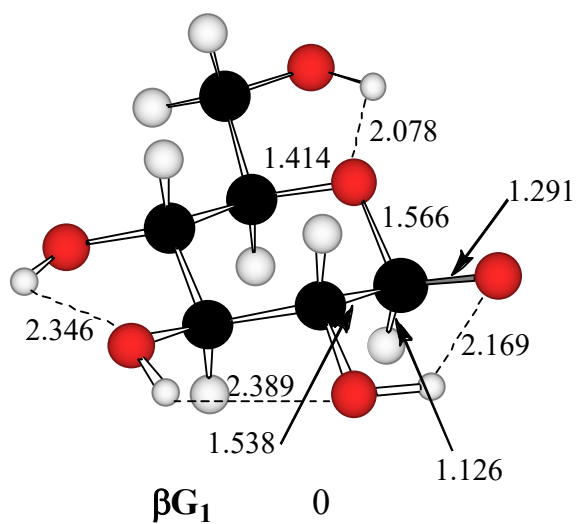


FIGURE 2

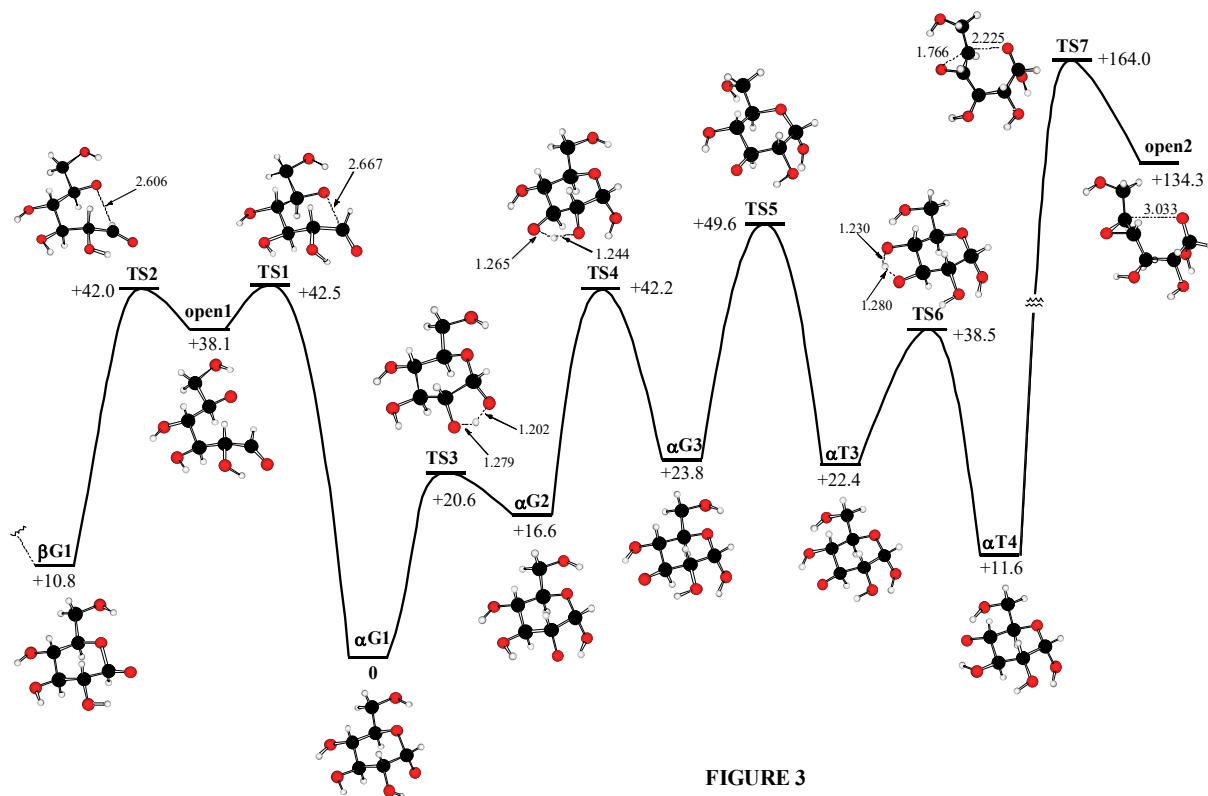


FIGURE 3

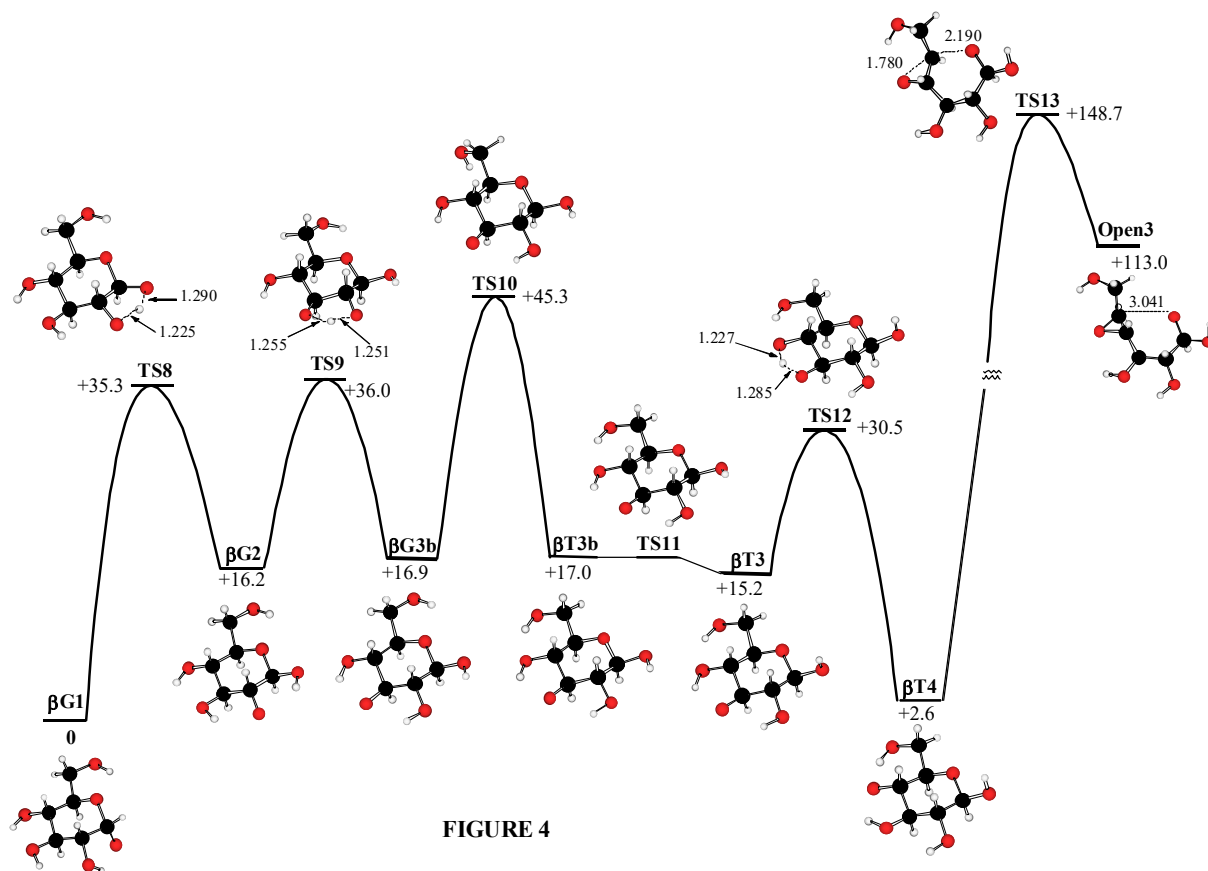
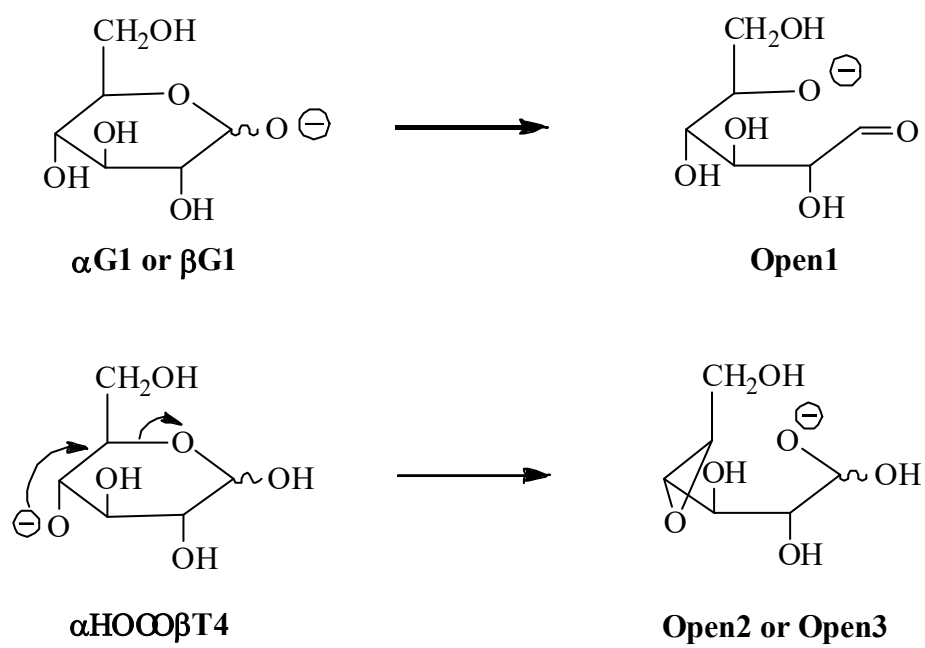


FIGURE 4



Scheme 1

Table 1 : Calculated enthalpies H°_{298} (Hartree), B3LYP and experimental deprotonation enthalpies $\Delta_{\text{acid}}H^\circ_{298}$ (kJ.mol⁻¹).

Structure	B3LYP/6-31+G(d,p)		B3LYP/6-311+G(2df,2p) //6-31+G(d,p)		B3LYP/6-311++G(2df,2pd) //6-31+G(d,p)		$\Delta_{\text{acid}}H^\circ_{298}$ (Experimental)
	H°_{298}	$\Delta_{\text{acid}}H^\circ_{298}$	H°_{298}	$\Delta_{\text{acid}}H^\circ_{298}$	H°_{298}	$\Delta_{\text{acid}}H^\circ_{298}$	
H ₂ O	-76.408972	1627.2	-76.437447	1632.8	-76.438425	1634.0	1634.9±0.2 ^(a) ; 1632.9±0.1 ^(b) ; 1634.7±0.4 ^(c) average value : 1634.2±0.2
OH ⁻	-75.791568		-75.817899		-75.818423		
CH ₃ OH	-115.679357	1588.5	-115.716411	1587.5	-115.717388	1588.8	1596.6±2.9 ^(a) ; 1597.9±2.3 ^(b) ; 1596±5 ^(c) average value : 1597±3
CH ₃ O ⁻	-115.076686		-115.114135		-115.114622		
C ₂ H ₅ OH	-154.972890	1574.8	-155.018975	1577.2	-155.020296	1578.2	1584.1±3.3 ^(a) ; 1584.6±3.2 ^(b) ; 1583±8 ^(c) average value : 1584±5
C ₂ H ₅ O ⁻	-154.375449		-154.420619		-154.421552		
NH ₃	-56.528796	1691.4	-56.548230	1689.9	-56.549036	1690.3	1690.3±1.7 ^(a) ; 1687.7±0.5 ^(b) ; 1690.2±3.3 ^(c) average value : 1689±2
NH ₂ ⁻	-55.886936		-55.906932		-55.907595		
CH ₃ NH ₂	-95.803435	1683.9	-95.831307	1681.7	-95.832338	1682.1	1687.0±3.3 ^(c)
CH ₃ NH ⁻	-95.164445		-95.193141		-95.194019		
$\bar{\Delta}^{(d)}$		5.9 (5.1)		4.6 (4.1)		3.9 (3.5)	

(a) Ref. 30. (b) Ref. 32 (c) Ref. 31 (d) Mean absolute standard deviation in kJ.mol⁻¹ (the values between brackets are obtained without considering ethanol).

Table2 : Total (Hartree), ZPE (kJ.mol⁻¹) and relative energies (kJ.mol⁻¹) of the different deprotonated structures of α -D-glucose.

Structure	Initial OH conformation	Final OH conformation	B3LYP/6-31G(d,p)			B3LYP/6-31+G(d,p)			B3LYP/6-311+G(2df,2p) //B3LYP/6-31+G(d,p)	
			E	ZPE	$\Delta E^{(a)}$	E	ZPE	$\Delta E^{(a)}$	E	$\Delta E^{(a)}$
αG1	G \bar{g} g \bar{g} g \bar{g} x	G \bar{g} g \bar{g} g \bar{g} x	-686.616724	484.1889	0	-686.679037	481.8567	0	-686.884761	0
αG-1	G \bar{g} g \bar{g} g \bar{g} x	G \bar{g} g \bar{g} g \bar{g} x	-686.616281	484.2421	1.2	-686.678218	481.9496	2.2	-686.884076	1.9
αT1	Tg \bar{g} g \bar{g} g \bar{g} x	Tg \bar{g} g \bar{g} g \bar{g} x	-686.614174	483.8396	6.3	-686.676726	481.8685	6.1	-686.882295	6.5
αG2	G \bar{g} g \bar{g} g \bar{x} t	G \bar{g} g \bar{g} g \bar{x} t	-686.610433	484.9510	17.3	-686.673179	482.8436	16.4	-686.878815	16.5
αG2b	G \bar{g} g \bar{g} x \bar{g}	G \bar{g} g \bar{g} x \bar{g}				-686.655898	480.7873	59.7	-686.862109	58.4
αG2c	G \bar{g} g \bar{g} x \bar{g}	G \bar{g} g \bar{g} x \bar{t}				-686.673189	482.8114	16.3	-686.878829	16.5
αG-2	G \bar{g} g \bar{g} x \bar{t}	G \bar{g} g \bar{g} x \bar{t}	-686.609824	484.9737	18.9	-686.671960	483.0639	19.8	-686.877713	19.7
αT2	Tg \bar{g} g \bar{x} t	Tg \bar{g} g \bar{x} t	-686.610119	484.9207	18.1	-686.672437	483.1789	18.7	-686.877876	19.4
αG3	G \bar{g} g \bar{x} t \bar{g}	G \bar{g} g \bar{x} t \bar{t}	-686.607461	485.7015	25.8	-686.670565	483.0460	23.4	-686.876130	23.9
αG-3	G \bar{g} g \bar{x} t \bar{g}	G \bar{g} g \bar{x} t \bar{t}	-686.605676	485.2672	30.1	-686.668152	482.9535	29.7	-686.873940	29.5
αT3	Tg \bar{g} x \bar{t} \bar{g}	Tg \bar{g} x \bar{t} \bar{t}	-686.609380	485.9437	21.0	-686.671515	483.6820	21.6	-686.876937	22.4
αT3b	Tg \bar{g} x \bar{t} \bar{g}	Tg \bar{g} x \bar{t} \bar{g}				-686.663229	482.9866	42.6	-686.869109	42.2
αT3c	Tg \bar{g} x \bar{t} \bar{t}	Tg \bar{g} x \bar{t} \bar{t}				-686.671529	484.1253	22.0	-686.877030	22.6
αG4	G \bar{g} x \bar{t} \bar{t} \bar{g}	G \bar{g} x \bar{t} \bar{t} \bar{t}	-686.598154	483.0418	47.6	-686.663246	481.4122	41.0	-686.868994	41.0
αG-4d	G \bar{g} x \bar{t} \bar{t} \bar{t}	G \bar{g} x \bar{t} \bar{t} \bar{t}	-686.595748	483.1528	54.0	-686.659895	481.2367	49.6	-686.866119	48.3
αT4	Tg \bar{x} \bar{t} \bar{t} \bar{t}	Tg \bar{x} \bar{t} \bar{t} \bar{t}	-686.613529	484.2551	8.5	-686.674626	482.2486	12.0	-686.880476	11.6
αT4b	Tg \bar{x} \bar{t} \bar{t} \bar{g}	Tg \bar{x} \bar{t} \bar{t} \bar{t}				-686.674626	482.3196	12.0	-686.880208	12.0
αT4c	Tg \bar{x} \bar{t} \bar{t} \bar{g}	Tg \bar{x} \bar{t} \bar{t} \bar{g}	-686.608158	482.3933	20.7	-686.670093	480.8977	22.5	-686.875955	22.2
αT4d	Tg \bar{x} \bar{t} \bar{g} \bar{g}	Tg \bar{x} \bar{t} \bar{g} \bar{g}				-686.670692	480.8254	20.9	-686.876479	20.7
αG6	Gx \bar{g} \bar{g} \bar{g} \bar{g}	Gx \bar{g} \bar{g} \bar{g} \bar{g}				-686.628170	477.0690	128.8	-686.834905	126.1
αT6	Tx \bar{g} \bar{g} \bar{g} \bar{g}	Tx \bar{g} \bar{g} \bar{g} \bar{g}				-686.655865	475.3769	54.4	-686.861944	53.4

(a) $\Delta E = [E(\text{XYnp}) - E(\alpha\text{G1})] \times 2625,50 + [ZPE(\text{XYnp}) - ZPE(\alpha\text{G1})]$

Table3 : Summary of the semi-empirical, ab initio and DFT relative energies (kJ.mol⁻¹) for the lowest energy structures of D-glucopyranose.

Structure	Relative energies (kJ/mol)				
	AM1 ^(a)	HF/6-31G(d) ^(a)	B3LYP/6-31G(d,p) ^(b)	B3LYP/6-31+G(d,p) ^(b)	B3LYP/6-311+G(2df,2p) //B3LYP/6-31+G(d,p) ^(b)
αG1	0	0	0	0	0
αG2	10.8	14.1	17.3	16.3	16.5
αT3	11.6		21.0	21.6	22.4
αT4	9.3	22.3	8.5	12.0	11.6
βG1	6.5	7.5	3.8	0	0
βG2	10.9		21.2	16.2	16.2
βT3	5.8	15.9	15.2	15.4	15.2
αT4	0	0	0	3.0	2.6

(a) From reference 13. (b) This work.

Table 4: Total (Hartree), ZPE (kJ.mol⁻¹) and relative energies (kJ.mol⁻¹) of the different deprotonated structures of β -D-glucose.

Structure	Initial OH conformation	Final OH conformation	B3LYP/6-31G(d,p)			B3LYP/6-31+G(d,p)			B3LYP/6-311+G(2df,2p) //B3LYP/6-31+G(d,p)	
			E	ZPE	$\Delta E^{(a)}$	E	ZPE	$\Delta E^{(b)}$	E	$\Delta E^{(b)}$
β G1	G \bar{g} g \bar{g} g \bar{g} x	G \bar{g} g \bar{g} g \bar{g} x	-686.609085	481.8643	3.8	-686.673982	480.0638	0.0	-686.879966	0.0
β G-1	G \bar{g} g \bar{g} g \bar{g} x	G \bar{g} g \bar{g} g \bar{g} x	-686.608513	481.8746	5.3	-686.672781	479.9339	3.0	-686.878867	2.8
β T1	Tg \bar{g} g \bar{g} g \bar{g} x	Tg \bar{g} g \bar{g} g \bar{g} x	-686.605696	481.7161	12.6	-686.670619	480.0722	8.8	-686.876548	9.0
β G2	G \bar{g} g \bar{g} x \bar{g}	G \bar{g} g \bar{g} x \bar{t}	-686.603255	483.9683	21.2	-686.668517	481.8800	16.2	-686.874494	16.2
β G2b	G \bar{g} g \bar{g} x \bar{g}	G \bar{g} g \bar{g} x \bar{g}				-686.655795	479.2477	46.9	-686.862319	45.5
β G2c	G \bar{g} g \bar{g} x \bar{t}	G \bar{g} g \bar{g} x \bar{t}				-686.668520	481.8734	16.2	-686.874497	16.2
β G-2	G \bar{g} g \bar{g} x \bar{g}	G \bar{g} g \bar{g} x \bar{t}	-686.602581	484.2176	23.2	-686.667132	482.1063	20.0	-686.873228	19.7
β T2	Tg \bar{g} g \bar{g} x \bar{g}	Tg \bar{g} g \bar{g} x \bar{t}	-686.602775	484.3780	22.9	-686.667321	482.3246	19.8	-686.873130	20.2
β G3	G \bar{g} g \bar{x} t \bar{g}	G \bar{g} g \bar{x} t \bar{g}	-686.603519	483.6258	20.2	-686.668392	481.5448	16.2	-686.874573	15.6
β G3b	G \bar{g} g \bar{x} t \bar{t}	G \bar{g} g \bar{x} t \bar{t}	-686.603485	483.6446	20.3	-686.667745	480.7884	17.1	-686.873810	16.9
β G-3	G \bar{g} g \bar{x} t \bar{g}	G \bar{g} g \bar{x} t \bar{g}	-686.601312	483.4986	25.9	-686.665416	481.0198	23.5	-686.871735	22.6
β T3	Tg \bar{g} x \bar{t} \bar{g}	Tg \bar{g} x \bar{t} \bar{g}	-686.605164	483.6370	15.9	-686.668865	482.0045	15.4	-686.874917	15.2
β T3b	Tg \bar{g} x \bar{t} \bar{t}	Tg \bar{g} x \bar{t} \bar{t}				-686.668149	481.5475	16.8	-686.874076	17.0
β T3c	Tg \bar{g} x \bar{t} \bar{g}	Tg \bar{g} x \bar{t} \bar{g}				-686.666342	481.7392	21.7	-686.872387	21.6
β G4	G \bar{g} x \bar{t} \bar{t} \bar{g}	G \bar{g} x \bar{t} \bar{t} \bar{g}	-686.594946	480.8693	39.9	-686.661651	479.5993	31.9	-686.868013	30.9
β G-4	G \bar{g} x \bar{t} \bar{t} \bar{g}	G \bar{g} x \bar{t} \bar{t} \bar{g}	-686.592016	480.9763	47.7	686.657592	479.4796	42.5	-686.864144	40.9
β T4	Tg \bar{x} \bar{t} \bar{t} \bar{g}	Tg \bar{x} \bar{t} \bar{t} \bar{g}	-686.610565	481.9400	0.0	-686.672975	480.3677	3.0	-686.879097	2.6
β T4b	Tg \bar{x} \bar{t} \bar{g} \bar{g}	Tg \bar{x} \bar{t} \bar{g} \bar{g}				-686.670399	480.4009	9.7	-686.876664	9.0
β T4c	Tg \bar{x} \bar{t} \bar{t} \bar{t}	Tg \bar{x} \bar{t} \bar{t} \bar{t}				-686.672241	480.6678	5.2	-686.878271	5.1
β T4d	Tg \bar{x} \bar{t} \bar{t} \bar{g}	Tg \bar{x} \bar{t} \bar{t} \bar{g}				-686.671945	479.9064	5.2	-686.878019	5.0
β G6	G \bar{x} g \bar{g} g \bar{g} \bar{g}	G \bar{x} g \bar{g} g \bar{g} \bar{g}				-686.626625	474.5294	118.8	-686.833810	115.7
β T6	G \bar{x} g \bar{g} g \bar{g} \bar{g}	T \bar{x} t \bar{g} g \bar{g} \bar{g}				-686.655797	473.7832	41.5	-686.862165	40.5

(a) $\Delta E = [E(\text{XYnp}) - E(\beta\text{T4})] \times 2625.50 + [\text{ZPE}(\text{XYnp}) - \text{ZPE}(\beta\text{T4})]$. (b) $\Delta E = [E(\text{XYnp}) - E(\beta\text{G1})] \times 2625.50 + [\text{ZPE}(\text{XYnp}) - \text{ZPE}(\beta\text{G1})]$

Table 5: Total (Hartree), ZPE (kJ.mol⁻¹) and relative energies (kJ.mol⁻¹) of the structures associated with D-glucopyranose ring-opening processes

Structure	B3LYP/6-31+G(d,p)			B3LYP/6-311+G(2df,2p)//B3LYP/6-31+G(d,p)	
	E	ZPE	ΔE	E	ΔE
αG1	-686.679037	481.8567	0.0	-686.884761	0.0
βG1	-686.673982	480.0638	11.5	-686.879966	10.8
TS1	-686.658981	473.9981	44.8	-686.865591	42.5
TS2	-686.658705	473.8121	45.3	-686.865692	42.0
Open1	-686.660265	473.4101	40.8	-686.867052	38.0
αT4	-686.674626	482.2486	0.0	-686.880476	0.0
TS3	-686.612308	472.3194	153.7	-686.818663	152.4
Open2	-686.622704	472.1309	126.2	-686.829889	122.7
βT4	-686.672975	480.3677	0.0	-686.879097	0.0
TS4	-686.612553	471.4435	149.7	-686.819047	148.7
Open3	-686.625911	472.1522	115.4	-686.832921	113.0

Table 6 : B3LYP/6-311+G(2df,2p)//B3LYP/6-31+G(d,p) $\Delta_{\text{acid}}H^{\circ}_{298}$ and $\Delta_{\text{acid}}G^{\circ}_{298}$ (kJ.mol⁻¹) of α - and β - anomers of D-glucose and deoxy-D-glucoses (see text for details).

Structure	$\Delta_{\text{acid}}H^{\circ}_{298}$	$\Delta_{\text{acid}}G^{\circ}_{298}$	$\Delta\Delta_{\text{acid}}H^{\circ}_{298}$ ^a	$\Delta\Delta_{\text{acid}}G^{\circ}_{298}$ ^a
α -D-glucose	1428.2	1398.3	0	0
β -D-glucose	1438.0	1408.4	<i>0</i>	<i>0</i>
α -2-deoxy-D-glucose	1468.2	1436.5	40.0	38.2
β -2deoxy-D-glucose	1469.5	1436.8	<i>31.5</i>	<i>28.4</i>
α -3deoxy-D-glucose	1443.8	1412.0	15.6	13.7
β -3deoxy-D-glucose	1452.0	1420.4	<i>14.0</i>	<i>12.0</i>
α -4deoxy-D-glucose	1438.8	1408.8	10.6	10.5
β -4deoxy-D-glucose	1447.4	1418.1	<i>10.5</i>	<i>9.7</i>
α -2OH-THP ^a	1522.2	1490.4	94.0	92.1
β -2OH-THP	1525.3	1493.4	87.3	85.0

a) 2-hydroxy-tetrahydropyran.

b) α -D-glucose and β -D-glucose taken as reference. Relative acidities for β - anomers are given in italic.